



An integrated on-line method for the preconcentration and simultaneous determination of metsulfuron methyl and chlorsulfuron using oxidized carbon nanotubes and second order fluorescent data

Carolina C. Acebal^{a,*}, Marcos Grünhut^{a,*}, Natalia E. Llamas^a, Matías Insausti^a, Lucie Zelená^b, Hana Sklenářová^b, Petr Solich^b, Beatriz S. Fernández Band^a

^a INQUISUR (UNS-CONICET), Department of Chemistry, Universidad Nacional del Sur, 1253 Alem Avenue, B8000CPB Bahía Blanca, Argentina

^b Department of Analytical Chemistry, Faculty of Pharmacy, Charles University, Heyrovského 1203, 500 05 Hradec Králové, Czech Republic

ARTICLE INFO

Article history:

Received 16 March 2016

Received in revised form 26 May 2016

Accepted 6 June 2016

Available online 07 June 2016

Keywords:

Sulfonylureas

Automated flow system

Oxidized multiwall carbon nanotubes

Photodegradation

Second order data algorithms

ABSTRACT

Trace amounts of two sulfonylurea herbicides widely used for crops protection, metsulfuron methyl (MSM) and chlorsulfuron (CSF) were simultaneously determined taking into account the different kinetic photodegradation behavior of their photoproducts in alkaline medium. As the analytes are present at trace concentration levels, a preconcentration by sorption on a mini-column packed with oxidized multiwall carbon nanotubes (ox-MWCNTs) at pH 3.0 was performed. The retained analytes were removed from the ox-MWCNTs mini-column with a mixture of ACN contained 10% (v/v) of NaOH pH 12.5. A total enrichment factor of 26-fold for a 14.50 mL sample volume was obtained. The eluate was photodegraded by UV radiation during 126 s and the fluorescent spectra corresponding to the analytes photoproducts were registered overtime between 300 and 500 nm. The kinetic second order data were analyzed by unfolded-partial least squares-residual bilinearization (U-PLS/RBL) and multidimensional-partial least squares-residual bilinearization (N-PLS/RBL) algorithms. The relative error of prediction (REP%) for N-PLS/RBL was 7.73% for MSM and 6.37% for CSF. In the case of U-PLS/RBL, this statistical parameter was 7.75% for MSM and 7.23% for CSF, respectively. The limits of detection (LOD) were 0.19 $\mu\text{g L}^{-1}$ for MSM and 1.14 $\mu\text{g L}^{-1}$ for CSF using N-PLS/RBL and 0.21 $\mu\text{g L}^{-1}$ for MSM and 1.03 $\mu\text{g L}^{-1}$ for CSF when U-PLS/RBL was applied.

The entire procedure was performed in an on-line integrated fully automated flow system coupled to a low mercury UV lamp (15 W, 254 nm) and a spectrofluorometer. In this manner, the preconcentration, photodegradation and detection steps were performed in a reproducible way.

After optimization, the method was successfully applied to the analysis of real water samples obtained in the south part of Buenos Aires province and used for irrigation and consumption.

© 2016 Elsevier B.V. All rights reserved.

1. Introduction

The sulfonylurea herbicides (SUHs) are a class of substituted urea herbicides used worldwide and, in particular, in the agricultural region surrounding the city of Bahía Blanca, Argentina. Potential routes of human exposure to these herbicides include consumption of contaminated food or drinking contaminated water. In particular, metsulfuron methyl (MSM) and chlorsulfuron (CSF) are two SUHs that can be found together in several commercial formulations (Alianza 75 WDG, Argus 75 WG, Finesse® WG and others), and their levels in water sources intended for both animal and human consumption must be monitored. Only allowable amounts of SUHs for drinking water are

established. Argentina's regulations stipulated a maximum concentration level of 100 $\mu\text{g L}^{-1}$ for total pesticides in water sources with conventional treatment [1].

Because MSM and CSF are usually present in complex matrices and has to be detected at low concentrations, the application of extraction and preconcentration procedures to perform the quantitative analysis of them is required.

The simultaneous determination of MSM and CSF using a solid-phase extraction (SPE) as an extraction approach and conventional sorbents (mainly C18) has been performed using different techniques. First attempts to determine both analytes were performed by gas chromatography [2], and by capillary electrophoresis [3]. Usually, high-performance liquid chromatography (HPLC) and ultra-high-performance liquid chromatography (UHPLC) have been the most extensively used techniques for these polar to middle polar and thermally labile compounds determination [4–6]. HPLC or UHPLC coupled with

* Corresponding authors.

E-mail addresses: cacebal@uns.edu.ar (C.C. Acebal), mgrunhut@uns.edu.ar (M. Grünhut).

mass spectrometry (MS) or tandem mass spectrometry (MS/MS) detection techniques, which have the advantages of improved sensitivity and high degree of selectivity, have been proven to be a powerful tool for the determination of trace levels of SUHs [7,8]. Additionally, a capillary electrophoresis method has been proposed by Springer et al. [9] as an alternative technique to achieve the separation and determination of these compounds using raw MWCNTs as a sorbent.

As a simple approach for the SUHs determination, their fluorescent behavior under UV irradiation in an aqueous micellar mobile phase was exploited. Since MSM and CSF are naturally non-fluorescent herbicides, their photochemical induced fluorescence signal was used to determine their concentrations either individually [10] or through the first-derivative of their binary mixtures [11]. Here, a flow injection analysis (FIA) system was proposed after off-line preconcentration employing successive liquid-liquid extraction steps.

Due to their outstanding chemical and physical properties, carbon nanotubes (CNTs) have been widely used in sorbent-based extraction techniques [12]. To the well-known advantages of using CNTs as sorbents, the benefits of automating conventional SPE procedure were provided. SPE procedure requires several steps to be performed in a reproducible way, and this characteristic can perfectly be achieved with the development of on-line preconcentration techniques. As expected, automation of SPE procedure allows minimize solvent and sample consumption, reduction of the analysis time and avoids exposure to potential hazards since the whole procedure takes place in a close system. Additionally, the quantity of sorbent that is employed when CNTs are used could be reduced compared to conventional sorbents used in SPE cartridges, leading to miniaturization of the process [13].

On the other hand, due to the sorption/desorption cycles, the compaction of CNTs in the packed column can occur leading to a decrease in the performance of the adsorption process and overpressure in the flow system. One interesting alternative, not only to enlarge their potential but also to enhance their solubility, is the functionalization of the CNTs surface by an acidic oxidative treatment. The oxidation process offers a larger number of oxygen containing functional groups, but also a more hydrophilic surface structure, which makes the CNTs more hydrophilic and suitable for sorption of moderately to polar compounds [14].

The increasing use of chemometrics in environmental studies over the last two decades corresponds to the intensive research dedicated to test and prove how powerful the data processing techniques can be in this field and also to the availability of appropriate software. Nevertheless, the spectroscopic measurement lacks of the required selectivity, particularly when similar chemical compounds must be analyzed in complex samples. The lack of selectivity or the presence of interfering species linked to natural samples demands the application of chemometric methods based on multivariate calibration techniques in order to overcome these limitations and to complement these analytical methodologies [15].

Multivariate calibration methods are focused on the establishment and application of mathematical models that relate to multivariate instrumental signals with analyte concentrations or sample properties [16]. The possibility to quantify an analyte in the presence of interferences, as long as the interfering compounds are present in the calibration samples during the establishment of the calibration model, is the so-called first-order advantage. The second-order advantage implies that the analyte contribution can be appropriately modelled, quantitatively estimated and resolved in the presence of unknown interferences, absent in the calibration samples [15]. The use of fluorescence and chemometric tools applied to the quantification of pesticides was demonstrated in the literature [17,18].

In a previous article, a flow-batch analysis (FBA) system to automate the preconcentration, photodegradation and fluorescent detection of MSM photoproducts in different water samples was developed. The SPE procedure was performed using a conventional sorbent (C18) and the photodegradation and detection were performed in a chamber [19].

The purpose of this work was to develop a fully automated flow manifold to achieve the simultaneous preconcentration and fluorescent determination of MSM and CSF by a chemometric approach taking into account the different kinetic photodegradation behavior of their photoproducts. The overlapped signals demand the use of algorithms that exploited the second order advantage, such as unfolded-partial least squares-residual bilinearization (U-PLS/RBL) and multidimensional-partial least squares-residual bilinearization (N-PLS/RBL). Because these analytes are present in environmental water samples in trace levels it is necessary to perform a preconcentration step. To accomplish this aim, an on-line SPE procedure was optimized using ox-MWCNTs as a novel sorbent for the selected analytes. The SPE mini-column was coupled to a reactor coiled around an UV lamp and photoproducts were then propelled to the spectrofluorometer to acquire the corresponding over time spectra. To the best of our knowledge, it is the first time that the different kinetics of photodegradation of MSM and CSF were studied and used to determine them simultaneously by a chemometric approach.

2. Experimental

2.1. Reagents

Metsulfuron methyl (MSM) and chlorsulfuron (CSF) were purchased from Sigma-Aldrich, Germany. A 140 mg L⁻¹ standard stock solution of each analyte was prepared in acetonitrile (≥99%, Merck, Germany, ACN) and stored in dark bottles at 4 °C. Calibration and validation set solutions were prepared daily by an appropriate dilution of the stock solutions with HCl pH 3.0.

All other solutions were prepared using analytical-grade reagents and ultra-pure water (18 MΩ cm⁻¹).

Nitric and sulfuric acids were obtained from Sigma-Aldrich (Germany). 50.0 mL NaOH (Merck, Germany) 0.10 mol L⁻¹ solution was prepared by dissolving a suitable amount of the solid drug in distilled water. A 0.03 mol L⁻¹ NaOH solution (pH 12.5) was prepared by diluting the concentrated solution. The pH of the samples was adjusted using a 0.01 mol L⁻¹ HCl (Merck, Germany) solution.

Multiwalled carbon nanotubes (MWCNTs) with average external diameter of 13–16 nm and purity >95% were provided by Bayer®. Before used, MWCNTs were dried at 80 °C for 2 h.

2.2. Apparatus and software

The spectrofluorometric measurements were performed on a Jasco® FP 6500 spectrofluorometer. The excitation wavelength was 276 nm and the emission spectra were recorded between 300 and 500 nm. The slit width for excitation and emission were 5 and 10 nm, respectively, and the photomultiplier tube (PMT) voltage was fixed to 475 V. The scan rate was 2000 nm min⁻¹. The fluids were pumped with a Gilson® Minipuls 3 peristaltic pump. A Hellma® 178–712-QS flow cell was used. NResearch® three-way solenoid valves were used to handle all the solutions in the system.

Tygon® tubes were used in all of the pumping channels. A tube with an i.d. of 1.14 mm was used for the ACN-NaOH mixture, whereas tubes with an i.d. of 1.30 mm were used for water, NaOH, air and sample. All the flow system connections were made of PTFE (0.5 mm i.d.). A lab-made photoreactor with a Philips® low mercury UV lamp (15 W, 254 nm) was used. In this device, 5.60 m of a PTFE tube was helically coiled around the UV lamp. An electronic actuator connected to a Pentium® 4 microcomputer was used to control the peristaltic pump, solenoid valves and the photoreactor. The software used to control the flow system was developed in the Labview® 5.1 visual programming language.

The infrared measurements were performed on a FTIR-NIR spectrometer Thermo Scientific Nicolet iS50.

Three-way array decomposition, fluorescence data processing and calibration was carried out by N-PLS/RBL and U-PLS/RBL using routines available in <http://www.iquir-conicet.gov.ar> in MatLab® R2010 environmental [20].

2.3. Preparation of ox-MWCNTs mini-column

In order to improve the solubility and decrease the aggregation of CNTs to avoid overpressure in the flow system, commercial MWCNTs were oxidized as have been reported in literature [21]. Briefly, 100 mg of purified MWNTs were mixed to 400 mL of a mixture of concentrated $\text{H}_2\text{SO}_4:\text{HNO}_3$ (3:1 by volume) acids used as an oxidant agent. The mixture was sonicated in an ultrasonic water bath (50 W, 70 Hz) during 5 h at the room temperature. Then, the obtained ox-MWCNTs were diluted with deionized water up to 2000 mL, filtered and washed with water until complete elimination of the residual acids was accomplished. After that, the ox-MWCNTs were left to dry at the room temperature during two days. To perform IR-spectra of MWCNTs and ox-MWCNTs, KBr tablets were prepared weighting 1.20 mg of raw MWCNTs or ox-MWCNTs, respectively, and mixed with 0.20 g of KBr. All the measurements were carried out at a wavenumbers range of 500–4000 cm^{-1} at the room temperature.

Finally, the mini-column was prepared by placing 60 mg of ox-MWCNTs into a cylindrical glass tube (3.5 cm length, 0.4 mm i.d.) using the dry packing method. To avoid losses of the sorbent material, cotton was used as frits and placed at both sides of the column. After packing, the mini-column was filled with a methanol solution and sonicated during 20 min to perform the dispersion of the ox-MWCNTs. Then, the column was washed with water for 10 min and with ACN for 5 min to remove impurities from packed sorbent.

2.4. Flow method

A flow system was performed to carry out the preconcentration, photodegradation and detection procedures. A schematic diagram of

the proposed flow system is shown in Fig. 1. The system consisted of five channels: C1, C2, C3, C4 and C5 that correspond to ACN-NaOH mixture, water, sample, air and NaOH, respectively. The flow rate for the C1 was 1.22 mL min^{-1} meanwhile the flow rate of the C2, C3, C4 and C5 was 1.37 mL min^{-1} . The direction of the flow for each channel was controlled by a three way solenoid valve. When the corresponding valve (i.e. V1, V2, V3, V4 and V5) was switched OFF, the fluid was recycled to the respective flask; when the valve was ON, the corresponding fluid was pumped toward the chemifold and through the ox-MWCNTs mini-column for V1, V2, V3 and V4, or to the photoreactor, in case of V5. Additionally, a filter (0.22 μm) was introduced in the C3 channel to filter the sample prior to the preconcentration step. A sixth valve (V6) was placed after the ox-MWCNTs mini-column. During the conditioning and loading steps, this valve was in the OFF position and thus the solutions passed through the ox-MWCNTs mini-column and were directed toward the waste. When this valve was ON, an appropriate volume of ACN-NaOH passed through the column to perform the elution of the analytes and then, the eluate was moved toward the photoreactor.

The ox-MWCNTs mini-column was washed with 3.60 mL of ACN and 2.30 mL of water. Thus, the V1 and V2 valves were sequentially switched ON for 177 s and 101 s, respectively. After this time, 14.50 mL of the standard solution or sample was pumped through the ox-MWCNTs minicolumn by switching the V3 valve to the ON position for 635 s, and the MSM and CSF were retained. Then, it was washed with 2.30 mL of water by witching the V2 valve to the ON position for 101 s. Before elution, ox-MWCNTs mini-column was dried by air during 180 s. Finally, the elution of MSM and CSF was performed using 0.55 mL of ACN-NaOH (90:10) solution. In this case, the V1 and V6 valves were switched to the ON position for 27 s. Simultaneously, the V5 valve was switched ON during 24 s and 0.55 mL of pH 12.5 NaOH solution was directed toward the chemifold to merge with the eluted solution. The eluted solution in alkaline medium was then directed toward the photoreactor. When the photoreactor was filled, the flow rate was reduced to 0.37 mL min^{-1} and the photoreactor was switched ON in

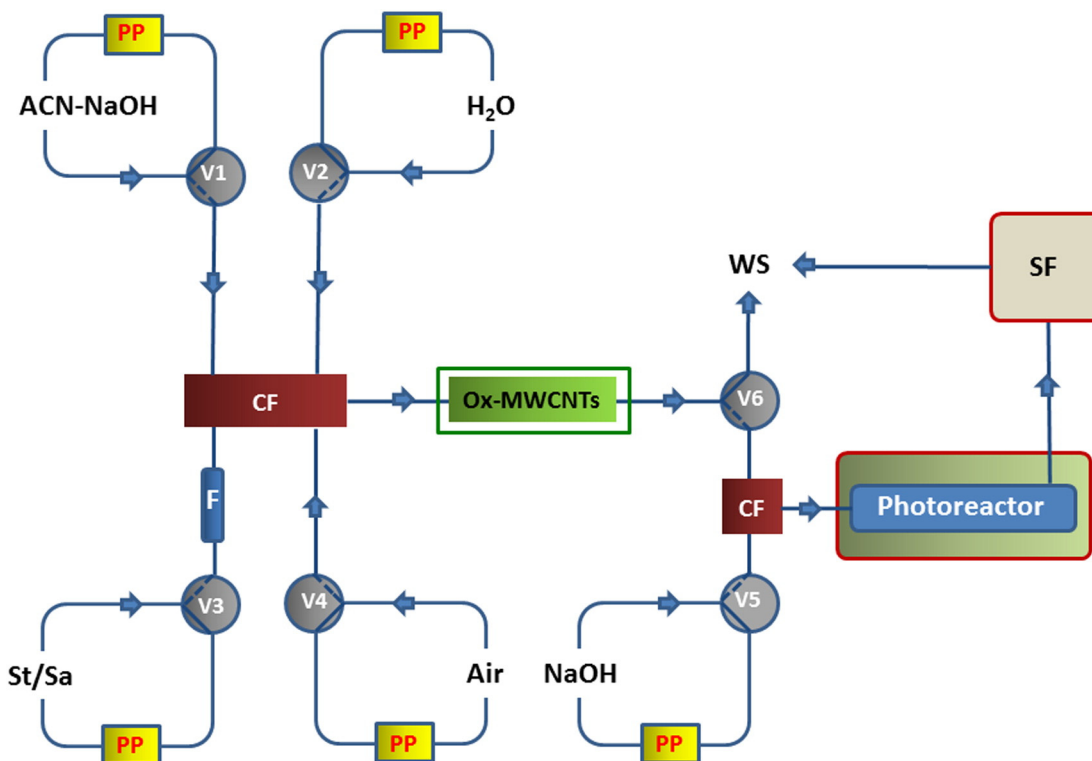


Fig. 1. Diagram of the flow system for preconcentration, photodegradation and simultaneous fluorescence detection of MSM and CSF. CF: chemifold; F: filter (0.22 μm); PP: peristaltic pump; SF: spectrofluorometer; V1–V6: solenoid valves; WS: waste.

order to perform the photodegradation of MSM and CSF. Immediately, spectra of the photoproducts were registered between 300 and 500 nm in the period of 28 s–126 s (98 s) every 7 s (i.e. in total 14 spectra). After this step, the solution was moved to the waste. Finally, the spectral data were arranged in matrices, pretreated and analyzed by U-PLS/RBL and N-PLS/RBL second order algorithms. Table 1 shows the switching time intervals and delivered volumes for the complete flow procedure.

2.5. Sampling and sample preparation

Different water sources used for animal and human consumption, agricultural irrigation and recreation, were sampled from the city of Bahía Blanca and the Villalonga town, both located in Buenos Aires region, Argentina.

One of the samples was collected from the Napostá Grande Creek situated at the north part of the region surrounding Bahía Blanca. Two samples were collected in Villalonga town: one was obtained from a water-well used for human consumption and the other from an irrigation channel. The fourth sample was tap water and was collected from our laboratory.

The collected samples were stored in the dark at 4 °C until the analysis was performed (no more than 48 h). The samples were properly homogenized and their pH value was adjusted to 3.0 with a 0.10 mol L⁻¹ HCl solution. Then, they were pre-filtered using 80 mm Whatman™ filter paper to remove sand and other solid particles. Afterwards, they were introduced into the flow system and filtered on-line with a 0.22 mm Whatman™ syringe filter before passing through the ox-MWCNTs mini-column.

2.6. Experimental design and data arrangement

2.6.1. Calibration set and real spiked samples

The calibration set was performed in accordance with a 2 × 2 full factorial design evaluating two factors: MSM and CSF concentrations, at two levels: 0.77 µg L⁻¹ and 7.70 µg L⁻¹ for MSM and 3.85 µg L⁻¹ and 38.5 µg L⁻¹ for CSF. The concentrations were selected taking into account the usual MSM-CSF ratio relation in the commercial products. Additionally, the calibration set included three replicates of the central point.

Table 1
Switching time intervals for the different steps of the continuous flow system.

Step	Switching time intervals (s)								
	V ₁	V ₂	V ₃	V ₄	V ₅	V ₆	PP	PR	SF
Filling channels									
All solutions	20	20	20	20	Off	20	On	Off	Off
Column conditioning									
ACN-NaOH	177	Off	Off	Off	Off	Off	On	Off	Off
Water	Off	101	Off	Off	Off	Off	On	Off	Off
Column loading									
Standard/sample	Off	Off	635	Off	Off	Off	On	Off	Off
Column washing									
Water	Off	101	Off	Off	Off	Off	On	Off	Off
Air	Off	Off	Off	180	Off	Off	On	Off	Off
Elution ^a									
ACN-NaOH	27	Off	Off	Off	24	27	On	Off	Off
pH conditioning ^a									
NaOH	27	Off	Off	Off	24	27	On	Off	Off
Photodegradation ^b	Off	Off	Off	Off	126	Off	On	On	Off
Detection ^b	Off	Off	Off	Off	98	Off	On	On	On

ACN: acetonitrile; V: solenoid valve; PP: peristaltic pump; PR: photoreactor; SF: spectrofluorimeter.

^a These steps were performed simultaneously.

^b These steps were performed simultaneously.

Real water samples obtained as mentioned in Section 2.5 were used to prepare the prediction set. The four environmental samples were spiked to perform a set of 20 prediction samples. Concentration levels were set according to a 2 × 2 full factorial design: 2.50 µg L⁻¹ and 5.96 µg L⁻¹ for MSM and 12.5 µg L⁻¹ and 29.8 µg L⁻¹ for CSF. The experiments corresponding to the calibration and prediction sets were performed in random order.

It is worth to notice that solutions of the calibration and validation sets were subjected to the whole procedure, included the preconcentration step, and processed in the same way as the real samples.

2.6.2. Data arrangement and pretreatment

Once the data is arranged in a matrix form for a set of samples, one alternative is to build a three way array that is a sensible choice when the data are trilinear. The data matrix was built as: sample by number of spectrum by emission wavelength. In this form, the calibration data set and the prediction data set were arranged in matrices of 11 × 14 × 200 and 20 × 14 × 200, respectively. Trilinearity of a three-way data array composed of data matrices for several samples requires that each data matrix is bilinear, and that both profiles for each constituent are the same in all samples.

The N-PLS/RBL and U-PLS/RBL algorithms may be used with trilinear data. The spectra were registered during approximately 2.4 s, so the beginning and the end of each spectrum corresponded to different time of photodegradation. But as they were recorded in completely repeatable way from sample to sample, identical profiles were found in each scanning [22]. Noteworthy, the time that the instrument requires to be ready for the next scanning in addition to the scanning process gives a total of approximately 7 s between each scan.

3. Results and discussion

3.1. Characterization of ox-MWNTs

The oxidation of CNTs allows the generation of carboxylic and hydroxyl groups on the CNTs surface leading to an increase of their solubility.

The FTIR spectra of raw and oxidized MWCNTs were compared where differences in transmittance signal among the samples of raw and acid-treated MWNTs can be observed. The spectra indicate intensive bands at wavenumbers of 3444 cm⁻¹ corresponding to the stretching vibrations of isolated surface –OH moieties and/or –OH in carboxyl groups. As a result of functionalization, the CO bands characteristic for carboxyl functional groups (–COOH) and of ketone/quinone are observed at 1718 and 1637 cm⁻¹, respectively. The increase in the amounts of hydrated surface oxides (H deformation and C stretching combination in surface phenols, hydroquinones and aromatic carboxylic acids) are observed on the increment of the intensity of the bands in the 1250–950 cm⁻¹ wavenumber region [23].

3.2. Selection of CNTs type

Zhou et al. have compared the performance of C18 and MWCNTs in the extraction and preconcentration of sulfonylurea herbicides [24]. On the other hand, Acebal et al. have performed the preconcentration of MSM using C18 as sorbent [19]. In this work, the retention characteristics of raw MWCNTs and ox-MWCNTs were evaluated to achieve an efficient extraction of MSM and CSF. For this purpose, two mini-columns were packed with the same quantity of the sorbents and standard solutions at concentration levels in the range of the experimental design were measured in triplicates according to the procedure listed in the Section 2.4.

Lower concentrations of both analytes could be measured and higher correlation coefficients were achieved when ox-MWCNTs were employed as a sorbent material. In comparison with the

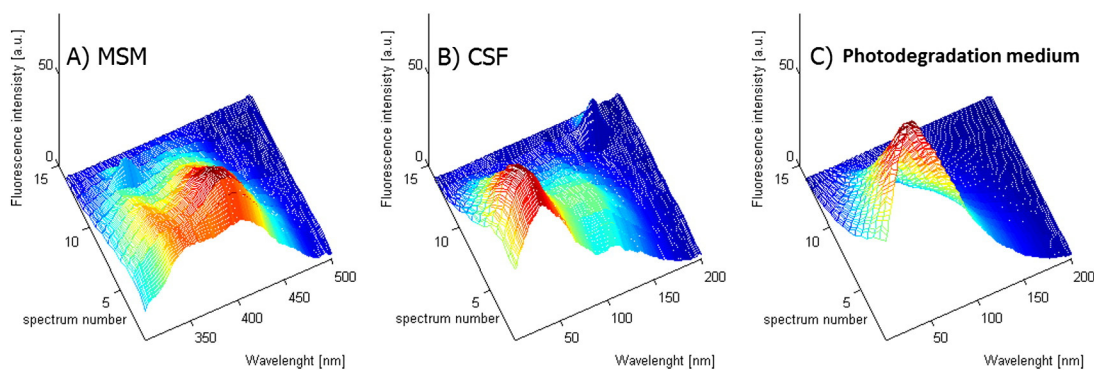


Fig. 2. 3D fluorescence spectra for solutions of MSM $4.23 \mu\text{g L}^{-1}$ (A), CSF $21.15 \mu\text{g L}^{-1}$ (B) and ACN-NaOH 90:10 (C).

preconcentration using C18, a similar enrichment factor was obtained after reducing the quantity of sorbent more than 3 times (200 mg of C18 vs 60 mg of ox-MWCNTs). Moreover, the baseline in the fluorescence measurements was improved meaning that the matrix effect was lower when ox-MWCNTs were used instead of raw MWCNTs and C18 as sorbents. Thus, ox-MWCNTs were selected for further experiments.

3.3. Effect of a pH on the analytes adsorption

The pH of the solutions has a significant influence on the retention of the analytes onto a CNTs surface since the ox-MWCNTs has a surface that contain oxygen groups. Thus, the surface charge depends on the pH of the surrounding solution. Taking into account the pKa values of MSM and CSF and the pH where the surface of ox-MWCNTs is not ionized, the effect of the pH of the sample solution on the retention of the analytes was studied between 2.0 and 3.0. It was observed that the retention of the analytes increased when the pH value was changed from 2.0 to 3.0 but slightly decreased when the pH value was further increased above 3.0. Hence, the pH of the sample was adjusted to 3.0.

3.4. Evaluation of parameters affecting the preconcentration performance

The optimization of the preconcentration parameters was based on obtaining the higher fluorescence signal and the repeatability of the measurements.

3.4.1. Optimization of the elution conditions

Some of the main characteristics of an eluent are effective release of the analyte in order to obtain acceptable recoveries and compatibility with the detection mode. The influence of different eluents on the photodegradation step and the fluorescence signal was exhaustively studied in a previous article [19]. Considering this, different ratios of a mixture of ACN (100 to 85%) and a pH 12.5 NaOH solution (0 to 15%) were tested in order to evaluate and compare the desorption of MSM and CSF from the ox-MWCNTs mini-column. Higher recoveries were obtained with ACN 100% and 90%. Even though similar results were achieved with both of them, the mixture of ACN-NaOH 90:10 was selected due to the higher repeatability obtained in fluorescence measurements.

The volume of the eluent was also optimized between 0.38 and 0.71 mL, keeping the volume of the sample and the final volumes used for the photodegradation and detection steps constant. Quantitative recoveries were obtained using 0.55 mL and this volume was used for further experiments. Considering the elution volume, an enrichment factor of 26-fold was achieved. It is worth to notice that for the fluorescence measurements, ratio of the sample and solvent-alkaline medium should be considered. For this reason, it was not possible to reduce the volume of eluent which can significantly improve the preconcentration.

3.4.2. Optimization of the sample loading volume

Generally, the increase in the volume of the sample is used to increase the extraction efficiency and reach the preconcentration of the

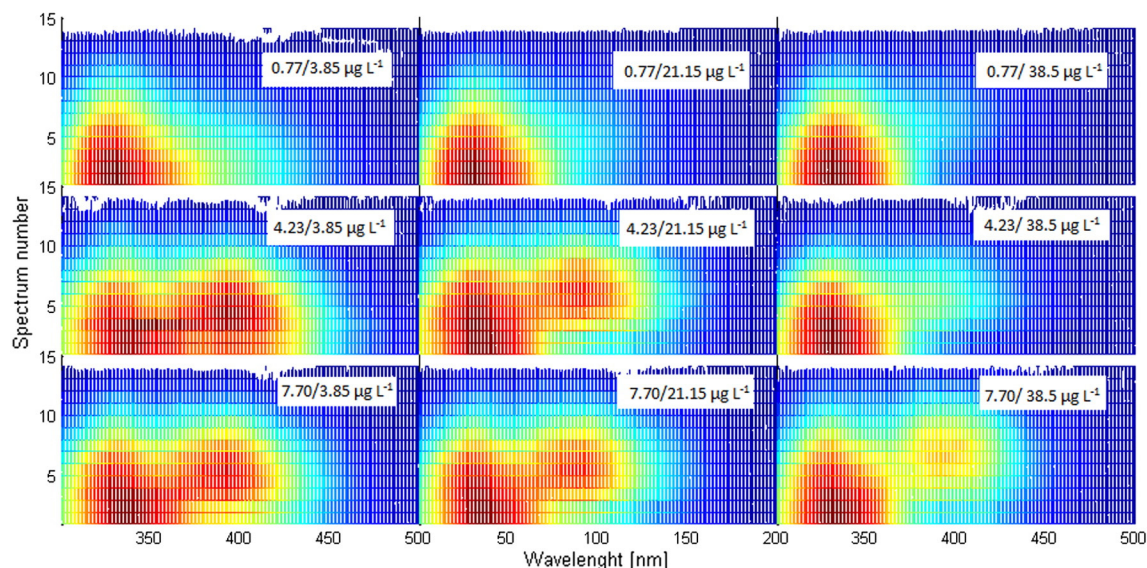


Fig. 3. Fluorescence spectra and concentrations (MSM/CSF) corresponding to the different samples of the calibration set.

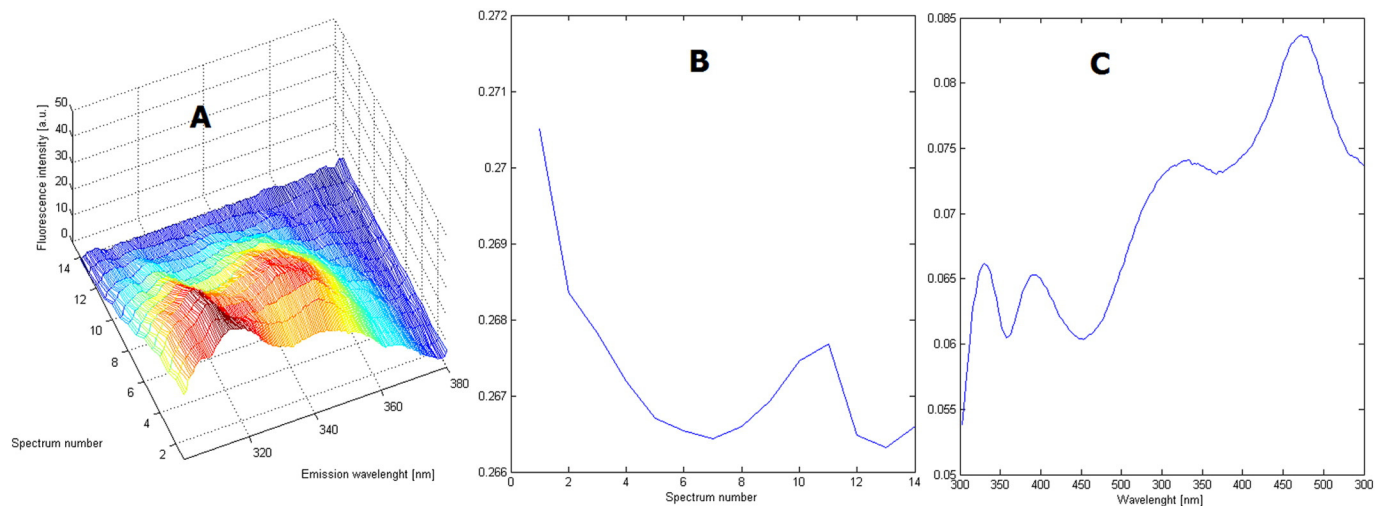


Fig. 4. A) Real spiked sample (S2.1); B) RBL profile in time mode; C) RBL profile in emission spectra mode.

compounds. But, as is well-known, too large sample volumes will not only enlarge the time of analysis but also could have a negative impact on the adsorption process.

To achieve the detection of low concentrations of both analytes with an adequate analysis time, the extraction on the ox-MWCNTs mini-column was evaluated in terms of sample loading volume between 4.35 mL and 28.32 mL. In this study, it was verified that the analytical signal progressively increased when the sample loading volume was incremented in the range from 4.35 to 14.50 mL, while it remained slightly constant at sample volumes over 14.50 mL.

Thus, 14.50 mL of the sample was passed through the ox-MWCNTs mini-column at the flow rate of 1.37 mL min^{-1} .

3.4.3. Optimization of the sample loading flow rate

The effect of the sample loading flow rate on the retention of MSM and CSF was tested between 0.69 and 2.06 mL min^{-1} . As this parameter is related to the contact time between the analytes and the sorbent, the fluorescence signal diminished when the loading flow rate was increased above 1.37 mL min^{-1} . Thus, this value was set as an optimum.

3.5. Conditions of the photodegradation study

The photodegradation behavior of MSM and CSF was previously studied taking into account the experimental conditions obtained by the authors in a preceding article [19]. In order to use compatible elution solvent and the photodegradation medium, ACN was chosen to perform the elution of the analytes from the ox-MWCNTs mini-column. In addition, the photodegradation must be performed in alkaline medium to form the photoproducts. Based on the highest fluorescence signal of the photoproducts and the best repeatability of the measurements, the optimum pH value of the NaOH solution was 12.5.

Considering this, a $4.23 \mu\text{g L}^{-1}$ MSM solution, $21.2 \mu\text{g L}^{-1}$ of CSF solution and their mixture were prepared in ACN-NaOH medium and photodegraded during five minutes. As can be expected, both analytes presented different photodegradation kinetics, which enable the use of chemometric approach for the spectral resolution.

3.6. Data analysis

The fluorescent spectra of MSM and CSF photoproducts as well as the photodegradation medium spectra (ACN-NaOH), were strongly overlapped. In order to distinguish the three constituents, the effect of UV irradiation has been studied. When the pesticides are irradiated, an increase and decrease of the fluorescence signal occur, without any shift of the maxima of emission.

Fig. 2 shows 3D spectra corresponding to of pure analytes (MSM and CSF) and the photodegradation medium (ACN-NaOH). As can be seen, during the irradiation, the photodegradation medium signal diminishes abruptly in comparison with the analytes fluorescent signals.

Fig. 3 shows the variation of the fluorescent intensities to the different pesticides concentrations corresponding to the calibration samples. It is necessary to remark that the fluorescence signals were not additive. Thus, the fluorescence of the mixture (at the different reactions times) was smaller than the sum of the individual fluorescence of the analytes, probably due to the effect of inner filter, because of the overlapping of the emission and excitation fluorescence maxima among sample components.

Table 2
Analysis of non-spiked and spiked real environmental water samples by N-PLS/RBL

Sample	MSM ($\mu\text{g L}^{-1}$)			CSF ($\mu\text{g L}^{-1}$)		
	Actual	Predicted	Recovery	Actual	Predicted	Recovery
S1	–	nd	–	–	nd	–
S1.1	2.50	2.59	103.7	12.50	12.13	97.0
S1.2	2.50	2.70	107.9	29.81	30.84	103.5
S1.3	5.96	5.34	89.5	12.50	12.93	103.5
S1.4	5.96	6.08	102.0	29.81	27.69	92.9
S2	–	nd	–	–	nd	–
S2.1	2.50	2.61	104.5	12.50	12.38	99.0
S2.2	2.50	2.60	104.1	29.81	29.46	98.8
S2.3	5.96	5.68	95.2	12.50	14.05	112.4
S2.4	5.96	5.48	92.0	29.81	30.34	101.8
S3	–	nd	–	–	nd	–
S3.1	2.50	2.30	92.0	12.50	12.31	98.5
S3.2	2.50	2.59	103.5	29.81	28.87	96.9
S3.3	5.96	5.59	93.7	12.50	13.30	106.4
S3.4	5.96	6.04	101.3	29.81	30.79	103.3
S4	–	nd	–	–	nd	–
S4.1	2.50	2.80	112.1	12.50	14.13	113.0
S4.2	2.50	2.50	100.2	29.81	29.78	99.9
S4.3	5.96	6.01	100.9	12.50	14.32	114.5
S4.4	5.96	5.94	99.6	29.81	27.88	93.5
Rec ^a ± sd			100.1 ± 6.2			102.1 ± 6.6
RMSEP ^b			0.275			1.076
REP ^c (%)			7.730			6.368

S1: Napostá Grande creek; S2: Villalonga water-well; S3: Villalonga irrigation channel; S4: tap water.

nd: the measured values are below the limit of quantification.

^a Rec: average recovery.

^b RMSEP: root mean square error prediction.

^c REP: relative error of prediction.

Table 3
Analysis of non-spiked and spiked real environmental water samples by U-PLS/RBL.

Sample	MSM ($\mu\text{g L}^{-1}$)			CSF ($\mu\text{g L}^{-1}$)		
	Actual	Predicted	Recovery	Actual	Predicted	Recovery
S1	–	nd	–	nd	–	–
S1.1	2.50	2.48	99.4	12.50	12.25	98.0
S1.2	2.50	2.67	106.8	29.81	28.86	96.8
S1.3	5.96	5.95	99.8	12.50	14.16	113.3
S1.4	5.96	5.80	97.3	29.81	28.86	96.8
S2	–	nd	–	nd	–	–
S2.1	2.50	2.83	113.3	12.50	12.53	100.3
S2.2	2.50	2.44	97.5	29.81	28.95	97.1
S2.3	5.96	5.74	96.4	12.50	14.14	113.2
S2.4	5.96	5.15	86.4	29.81	30.12	101.0
S3	–	nd	–	nd	–	–
S3.1	2.50	2.28	91.1	12.50	12.29	98.3
S3.2	2.50	2.46	98.6	29.81	27.23	91.3
S3.3	5.96	5.57	93.4	12.50	13.49	107.9
S3.4	5.96	6.19	103.8	29.81	29.63	99.4
S4	–	nd	–	nd	–	–
S4.1	2.50	2.90	116.1	12.50	14.06	112.5
S4.2	2.50	2.48	99.3	29.81	29.63	99.4
S4.3	5.96	5.86	98.3	12.50	14.15	113.2
S4.4	5.96	5.81	97.4	29.81	27.67	92.8
Rec ^a \pm sd			99.7 \pm 7.5			102.0 \pm 7.5
RMSEP ^b			0.276			1.222
REP ^c (%)			7.755			7.228

S1: Napostá Grande creek; S2: Villalonga water-well; S3: Villalonga irrigation channel; S4: tap water.

nd: the measured values are below the limit of quantification.

^a Rec: average recovery.

^b RMSEP: root mean square error prediction.

^c REP: relative error of prediction.

3.7. Analytical performance and application to real samples

The first step in the application of N-PLS/RBL and U-PLS/RBL was the assessment of the optimum number of calibration factors (A). This was done by resorting to the leave-one-out cross-validation procedure, which computes the ratios $F(A) = \text{PRESS}(A < A^*) / \text{PRESS}(A)$; where PRESS is the predicted error sum of squares, A is a trial number of factors and A^* corresponds to the minimum PRESS. The number of optimum factors was selected taking into account the one leading to a probability of less than 75% and $F > 1$. Since the present study was carried out with 2

analytes in a photodegradation medium with fluorescent signal, an additional latent variable was necessary in order to model the variability of the data, so A was equal to 3.

The next step was to estimate the number of unexpected components in the prediction set via the post-calibration RBL procedure. The success of RBL in extracting a spectral contribution of an unknown component from the samples was demonstrated by the good agreement among the predicted and experimental profiles of the analytes (Fig. 4). Every sample of the prediction set was estimated separately by means of the calculation of a model using the whole calibration set and one of the prediction samples at a time. The analysis of real samples would not be possible if the second order advantage was not present. The calibration was evaluated with synthetic mixtures of MSM, CSF, ACN, NaOH and water, but the real samples contain some fluorescent compounds not included in the calibration process. Using three factors and one RBL to model calculations, the RBL founded was the summary of the fluorescent signals of unknown compounds. Fig. 4 shows the profile recovered by RBL process, and a spectrum of one real spiked sample. The differences with the synthetic samples can be observed on the fluorescent signals at the beginning of registration, where the first four spectra of every sample showed a high contribution of unknown compounds. Without this extra profile decomposition, the correct quantification of the real samples would not be possible.

In the prediction of low concentrations samples of MSM modelled with N-PLS/RBL, the limit of detection (LOD) obtained using $3.3 \times$ standard deviation was $0.19 \mu\text{g L}^{-1}$ and the limit of quantification (LOQ) obtained using $10 \times$ standard deviation was $0.58 \mu\text{g L}^{-1}$ [26]; and considering low concentration samples of CSF the LOD was $1.14 \mu\text{g L}^{-1}$ and the LOQ was $3.44 \mu\text{g L}^{-1}$. Using the U-PLS/RBL algorithm, the LOD and LOQ for MSM were $0.21 \mu\text{g L}^{-1}$ and $0.64 \mu\text{g L}^{-1}$, respectively, meanwhile for CSF, the LOD and LOQ were $1.03 \mu\text{g L}^{-1}$ and $3.11 \mu\text{g L}^{-1}$, respectively.

The statistical parameters and the results, obtained in the analysis of the real samples and spiked real samples, are collected in Tables 2 and 3. The results obtained for the two analytes are acceptable for both algorithms employed.

The elliptical joint confidence regions (EJCR) of the regression of predicted versus nominal concentrations in the prediction set was studied for the two second-order calibration methods [25]. The corresponding plots are shown in Fig. 5. All confidence regions contain the ideal

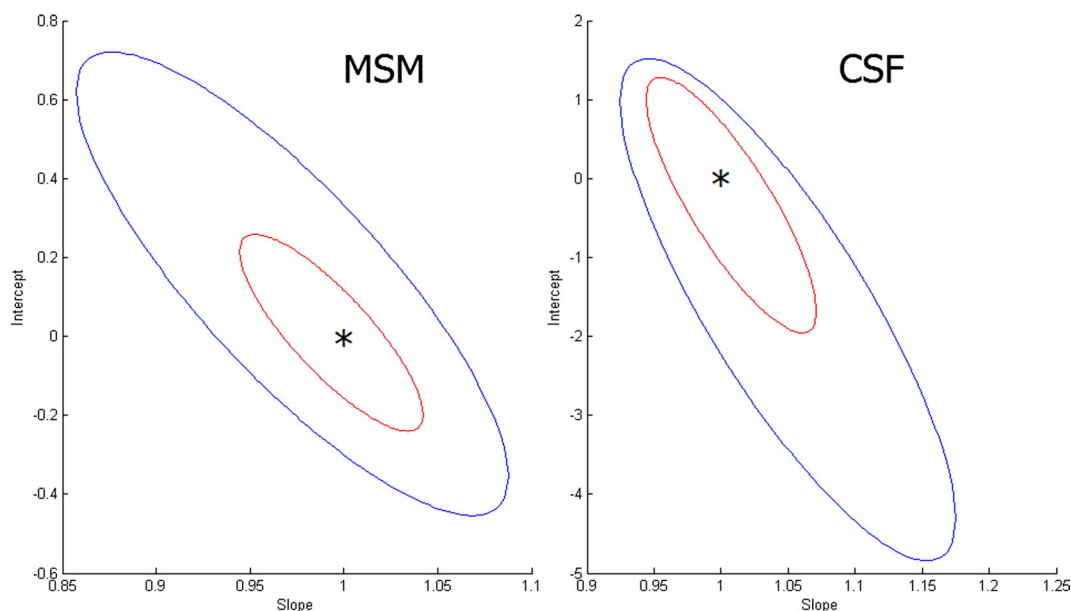


Fig. 5. Elliptical joint confidence regions (EJCR) for MSM and CSF predictions. Red: EJCR for NPLS/RBL, Blue: EJCR for U-PLS/RBL. (For interpretation of the references to color in this figure legend, the reader is referred to the web version of this article.)

point of unit slope and zero intercept (indicating accuracy), and the elliptic sizes obtained with N-PLS are slightly lower, suggesting that this chemometric methodology show higher predictive ability than U-PLS.

As was indicated before, and considering Argentina's allowable maximum level of pesticides in water sources for human consumption with conventional treatment, the proposed method is adequate for determining MSM and CSF levels in the analyzed samples.

4. Conclusions

This study describes a very attractive integrated automated method to perform the simultaneous quantification of trace levels of metsulfuron methyl and chlorsulfuron in environmental water samples. Taking account the established requirements of the Argentine legislation and the low concentrations usually founded in water samples, a preconcentration step is required. For the first time, ox-MWCNTs were tested as sorbent for the on-line SPE procedure of the target analytes. The evaluation of the retention efficiency showed that ox-MWCNTs were adequate sorbents to perform the preconcentration of both analytes under the conditions required to be coupled to the photodegradation step. Furthermore, the use of ox-MWCNTs allowed to decrease the overpressure in the flow system and avoided the compaction of the sorbent material owing to their higher solubility compared with raw MWCNTs.

Due to the difference in the kinetic photodegradation of MSM and CSF, the quantification of both analytes was possible by using emission fluorescent spectra as a function of the photo-irradiation time. The use of N-PLS/RBL and U-PLS/RBL was the key to model this type of second order data and to achieve good prediction results in real samples that have fluorescent signals not included in calibration samples. Based on the obtained analytical parameters (REP%, LOD and LOQ) and the recoveries percentages, the proposed method assisted by chemometric tools have presented an acceptable analytical performance to determine trace level of MSM and CSF in the analyzed samples.

Acknowledgments

The authors gratefully acknowledge financial support of the Bilateral Cooperation between Argentina and the Czech Republic, Project no. ARC/13/09 (7AMB14AR029). C. Acebal, M. Grünhut, N. Llamas, M. Insausti and B. Fernandez Band also would like to express their gratitude to Universidad Nacional del Sur (PGI 24/Q054) and CONICET (PIP 11220120100625KE5). L. Zelená acknowledged support by the Project of specific research, SVV No. 260292.

References

- [1] Ley 24051, Decreto 831, Régimen de desechos peligrosos, Anexo II, Tabla I.
- [2] P. Klaffenbach, P. Holland, Analysis of sulfonylurea herbicides by gas-liquid chromatography. 2. Determination of chlorsulfuron and metsulfuron-methyl in soil and water samples, *J. Agric. Food Chem.* 41 (1993) 396–401.
- [3] G. Dinelli, A. Vicari, P. Catizone, Use of capillary electrophoresis for detection of metsulfuron and chlorsulfuron in tap water, *J. Agric. Food Chem.* 41 (1993) 742–746.
- [4] Q. Wu, C. Wang, Z. Liu, C. Wu, X. Zeng, J. Wen, Z. Wang, Dispersive solid-phase extraction followed by dispersive liquid-liquid microextraction for the determination

- of some sulfonylurea herbicides in soil by high-performance liquid chromatography, *J. Chromatogr. A* 1216 (2009) 5504–5510.
- [5] S. Seccia, S. Albrizio, P. Fidente, D. Montesano, Development and validation of a solid-phase extraction method coupled to high-performance liquid chromatography with ultraviolet-diode array detection for the determination of sulfonylurea herbicide residues in bovine milk samples, *J. Chromatogr. A* 1218 (2011) 1253–1259.
- [6] G. Fang, J. Chen, J. Wang, J. He, S. Wang, *N*-methylimidazolium ionic liquid-functionalized silica as a sorbent for selective solid-phase extraction of 12 sulfonylurea herbicides in environmental water and soil samples, *J. Chromatogr. A* 1217 (2010) 1567–1574.
- [7] C. Yan, B. Zhang, W. Liu, F. Feng, Y. Zhao, H. Du, Rapid determination of sixteen sulfonylurea herbicides in surface water by solid phase extraction cleanup and ultra-high-pressure liquid chromatography coupled with tandem mass spectrometry, *J. Chromatogr. B* 879 (2011) 3484–3489.
- [8] M.C. Hurtado-Sánchez, R. Romero-González, M.I. Rodríguez-Cáceres, I. Durán-Merás, A. Garrido Frenich, Rapid and sensitive on-line solid phase extraction-ultra high performance liquid chromatography-electrospray-tandem mass spectrometry analysis of pesticides in surface waters, *J. Chromatogr. A* 1305 (2013) 193–202.
- [9] V.H. Springer, A.G. Lista, A simple and fast method for chlorsulfuron and metsulfuron methyl determination in water samples using multiwalled carbon nanotubes (MWCNTs) and capillary electrophoresis, *Talanta* 83 (2010) 126–129.
- [10] A. Coly, J.J. Aaron, Sensitive and rapid flow injection analysis of sulfonylurea herbicides in water with micellar-enhanced photochemically induced fluorescence detection, *Anal. Chim. Acta* 392 (1999) 255–264.
- [11] A. Coly, J.J. Aaron, Simultaneous determination of binary mixtures of sulfonylurea herbicides in water by first-derivative photochemically induced spectrofluorimetry, *J. AOAC International* 84 (2001) 1745–1750.
- [12] R. Lucena, B. Simonet, S. Cárdenas, M. Valcárcel, Potential of nanoparticles in sample preparation, *J. Chromatogr. A* 1218 (2011) 620–637.
- [13] C. Acebal, B. Simonet, M. Valcárcel, Nanoparticles and continuous-flow systems combine synergistically for preconcentration, *Trends Anal. Chem.* 43 (2013) 109–120.
- [14] K. Pyrzynska, Carbon nanostructures for separation, preconcentration and speciation of metal, *Trends Anal. Chem.* 29 (2010) 718–727.
- [15] S. Mas, A. de Juan, R. Tauler, A.C. Olivieri, G.M. Escandar, Application of chemometric methods to environmental analysis of organic pollutants: a review, *Talanta* 80 (2010) 1052–1067.
- [16] R. Bro, Multivariate calibration: what is in chemometrics for the analytical chemist? *Anal. Chim. Acta* 500 (2003) 185–194.
- [17] S.-H. Zhu, H.-L. Wu, A.-L. Xia, J.-F. Nie, Y.-C. Bian, C.-B. Cai, R.-Q. Yu, Excitation-emission-kinetic fluorescence coupled with third-order calibration for quantifying carbaryl and investigating the hydrolysis in effluent water, *Talanta* 77 (2009) 1640–1646.
- [18] M.L. Nahorniak, G.A. Cooper, Y.-C. Kim, K.S. Booksh, Three- and four-way parallel factor (PARAFAC) analysis of photochemically induced excitation-emission kinetic fluorescence spectra, *Analyst* 130 (2005) 85–93.
- [19] C. Acebal, M. Grünhut, I. Šrámková, P. Chocholouš, A. Lista, H. Sklenářová, P. Solich, B. Fernández Band, Application of a fully integrated photodegradation-detection flow-batch analysis system with an on-line preconcentration step for the determination of metsulfuron methyl in water samples, *Talanta* 129 (2014) 233–240.
- [20] MATLAB, The Mathworks, Inc., Natick, MA, USA.
- [21] X. Xiong, J. Ouyang, W.R.G. Baeyens, J.R. Delanghe, X. Shen, Y. Yang, Enhanced separation of purine and pyrimidine bases using carboxylic multiwalled carbon nanotubes as additive in capillary zone electrophoresis, *Electrophoresis* 27 (2006) 3243–3253.
- [22] A.C. Olivieri, G.M. Escandar, *Practical Three-Way Calibration* Ed. Elsevier, The Netherlands, 2014.
- [23] L. Stobinski, B. Lesiak, L. Kövér, J. Tóth, S. Biniak, G. Trykowski, J. Judek, Multiwall carbon nanotubes purification and oxidation by nitric acid studied by the FTIR and electron spectroscopy methods, *J. Alloys Compd.* 501 (2010) 77–84.
- [24] Q. Zhou, J. Xiao, W. Wang, Comparison of multiwalled carbon nanotubes and a conventional adsorbent on the enrichment of sulfonylurea herbicides in water samples, *Anal. Sci.* 23 (2007) 189–192.
- [25] J. Riu, F.X. Rius, Method comparison using regression with uncertainties in both axes, *Trends Anal. Chem.* 16 (1997) 211–216.
- [26] A.C. Olivieri, H.-L. Wu, Y. Ru-Qin, MVC2: a MATLAB graphical interface toolbox for second-order multivariate calibration, *Chemom. Intell. Lab. Syst.* 96 (2009) 246–251.